Crystal Structure of a Catalytic Site Mutant of β-Amylase from *Bacillus cereus* var. *mycoides* Cocrystallized with Maltopentaose

Hideo Miyake,[‡] Genji Kurisu,[§] Masami Kusunoki,[§] Sigenori Nishimura,[‡] Shinichi Kitamura,[‡] and Yasunori Nitta*[,‡]

Graduate School of Agriculture and Biological Sciences, Osaka Prefecture University, Sakai, Osaka 599-8531, Japan, and Institute for Protein Research, Osaka University, Suita, Osaka 565-0871, Japan

Received December 26, 2002; Revised Manuscript Received February 24, 2003

ABSTRACT: The X-ray crystal structure of a catalytic site mutant of β-amylase, E172A (Glu172 → Ala), from *Bacillus cereus* var. *mycoides* complexed with a substrate, maltopentaose (G5), and the wild-type enzyme complexed with maltose were determined at 2.1 and 2.0 Å resolution, respectively. Clear and continuous density corresponding to G5 was observed in the active site of E172A, and thus, the substrate, G5, was not hydrolyzed. All glucose residues adopted a relaxed $^4C_1$ conformation, and the conformation of the maltose unit for Glc2 and Glc3 was much different from those of other maltose units, where each glucose residue of G5 is named Glc1−Glc5 (Glc1 is at the nonreducing end). A water molecule was observed 3.3 Å from the C1 atom of Glc2, and 3.0 Å apart from the OE1 atom of Glu367 which acts as a general base. In the wild-type enzyme−maltose complex, two maltose molecules bind at subsites −2 and −1 and at subsites +1 and +2 in tandem. The conformation of the maltose molecules was similar to that of the condensation product of soybean β-amylase, but differed from that of G5 in E172A. When the substrate flips between Glc2 and Glc3, the conformational energy of the maltose unit was calculated to be 20 kcal/mol higher than that of the *cis* conformation by MM3. We suggest that β-amylase destabilizes the bond that is to be broken in the ES complex, decreasing the activation energy, $\Delta G^{\ddagger}$, which is the difference in free energy between this state and the transition state.

β-Amylase (EC 3.2.1.2) hydrolyzes the α-1,4-glucosidic linkage of α-1,4-D-glucans, such as starch, thereby liberating β-maltose from the nonreducing end of the substrate. β-Amylase belongs to family 14 (*1*) and is distributed throughout higher plants and certain bacteria. The level of sequence homology between them is low (30−40%), although some regions in the sequence are conserved among all β-amylases (*2*). The subsite structures of β-amylase have been determined for soybean, wheat bran, and *Bacillus cereus* (*3*−*6*). The three-dimensional structures of β-amylase from soybean (*7*−*9*), sweet potato (*10*), a 7-fold mutant of barley (*11*), and *B. cereus* (*12*−*14*) have been reported. The active site is located in the catalytic domain (domain A), which consists of a $(\beta/\alpha)_8$ barrel, and is constructed with many conserved amino acid residues. But a region of the C-terminus differs between plant and bacterial β-amylases, with bacterial β-amylases possessing a starch binding domain which exhibits a fold similar to those of cyclodextrin glycosyltransferase (CGTase)[1] (*15*) and glucoamylase (*16*).

We previously demonstrated that one of the catalytic residues of soybean β-amylase is the carboxyl group of Glu186, by using 2,3-epoxypropyl α-D-glucopyranoside (α-EPG) as an affinity labeling reagent for β-amylase (*17*, *18*). On the basis of the structure of soybean β-amylase in complex with maltose, Mikami et al. pointed out that two glutamic acid residues (Glu186 and Glu380) of soybean β-amylase behave as the catalytic groups (*8*). In the case of β-amylases from *B. cereus*, Oyama et al. and Mikami et al. have reported that Glu172 and Glu367 are the catalytic residues and correspond to Glu186 and Glu380 of soybean β-amylase, respectively (*12*, *13*). Oyama et al. determined crystal structures of *Bacillus cereus* var. *mycoides* β-amylase (abbreviated as BCM β-amylase) complexed with α-EPG or 3,4-epoxybutyl α-D-glucopyranoside (α-EBG) (*14*), and found that the affinity labeling reagents were covalently bound to Glu172. On the other hand, we recently argued that Glu172 is a proton donor and Glu367 acts as a general base, based on the chemical rescue of the hydrolytic activity of a catalytic site mutant [E367A (Glu367 → Ala)] by azide (*19*). To clarify the mechanism of substrate hydrolysis, we need to know the manner of binding of a substrate, such as maltooligosaccharide, to the active site of the enzyme. Such structural studies have not been reported for β-amylase, though they have been for α-amylase (*20*−*22*) and CGTase (*23*−*26*).

In the previous study, we created a catalytic residue mutant [E172A (Glu172 → Ala)] of BCM β-amylase by site-directed mutagenesis (*19*). In the study presented here, we have successfully obtained crystals of E172A complexed with G5

* To whom correspondence should be addressed: Graduate School of Agriculture and Biological Sciences, Osaka Prefecture University, Sakai, Osaka 599-8531, Japan. Telephone: 81 (72) 254-9473. Fax: 81 (72) 254-9474. E-mail: nitta@biochem.osakafu-u.ac.jp.

[‡] Osaka Prefecture University.

[§] Osaka University.

[1] Abbreviations: CGTase, cyclodextrin glycosyltransferase (EC 2.4.1.19); α-EPG, 2,3-epoxypropyl α-D-glucopyranoside; BCM, *Bacillus cereus* var. *mycoides*; α-EBG, 3,4-epoxybutyl α-D-glucopyranoside; GGX, *O*-α-D-glucopyranosyl-(1→4)-*O*-α-D-glucopyranosyl-(1→4)-D-xylopyranose; BQ10-S1, *B. cereus* BQ10-S1 SpoII; F_o and F_c, observed and calculated X-ray structure factor amplitudes, respectively; *R*-factor, X-ray residual factor; *B*-factor, X-ray temperature factor.

10.1021/bi020712x CCC: $25.00
Published on Web 04/18/2003

(E172A−G5 complex) and the wild-type enzyme complexed with maltose (wild-type enzyme−maltose complex), and the crystal structures were determined at 2.1 and 2.0 Å resolution, respectively, by X-ray crystal structure analysis. The conformation of G5 bound at the active site in the E172A−G5 complex was revealed. We discuss the mechanism for the hydrolysis of the substrate on the basis of the conformation of the substrate bound at the active site and the active site environment surrounding it.

MATERIALS AND METHODS

Enzyme Preparation and Crystallization. The preparation of recombinant BCM β-amylase (wild-type enzyme) and the E172A mutant has been described previously (*19*). The wild-type enzyme complexed with maltose and the E172A mutant complexed with maltopentaose (G5) were crystallized by the hanging drop vapor diffusion method (*27*). A crystallization drop, which contained a mixture of 2 μL of protein solution containing 15 mg/mL protein in 100 mM acetate buffer (pH 4.6) and 2 μL of precipitant solution containing 16−18% (w/v) PEG 6000, 7% (w/v) ammonium sulfate, and 50 mM maltose or G5 as a ligand in 100 mM acetate buffer (pH 4.6), was equilibrated against 0.45 mL of precipitant solution at 293 K. A stack of thin-plate crystals grew after 1 week. To obtain larger and single crystals, a microseeding technique (*28*) was used. Crystals grew within 2 weeks to a size of up to 0.4 mm × 0.2 mm × 0.2 mm.

Data Collection and Structure Determination. X-ray data of each complex were collected with a Quantum4R two by two array CCD detector consisting of four modules (Area Detector Systems Corp.) with synchrotron radiation with a wavelength of 1.0000 Å at beamline BL-18B of the Photon Factory operated at 2.5 GeV at the High Energy Accelerator Research Organization (Tsukuba, Japan). A crystal of each complex was soaked in precipitant solution containing 29% glycerol before diffraction data collection, followed by soaking in liquid nitrogen, and then it was placed in a nitrogen gas stream and its temperature maintained at 100 K. Data were processed with DPS/MOSFLM (*29*) and SCALA in the CCP4 package (*30*).

The crystal structures were determined by the molecular replacement method using the program AmoRe (*31*) in the CCP4 package, and using the crystal structure of free BCM β-amylase (PDB entry 5BCA) (*12*) as the search model. Refinements were carried out with CNS (*32*). Five percent of the refractions were set aside for R_{free} calculations (*33*). The molecular models were built using O (*34*) based on $2F_o - F_c$ and $F_o - F_c$ electron density maps, and were improved through many steps by alternate cycles of model building and crystallographic refinement with CNS. The results of data collection and refinement statistics are summarized in Table 1.

The coordinates and structure factors of the E172A−G5 complex (PDB entry 1ITC) and the wild-type enzyme−maltose complex (PDB entry 1J18) have been deposited in the Protein Data Bank.

RESULTS AND DISCUSSION

Structure of E172A Complexed with Maltopentaose. Crystal structures of β-amylases complexed with substrate analogues have been determined by X-ray crystallography (*7*−*14*). However, the structure complexed with the substrate has not been analyzed. In the study presented here, we could determine the structure of a catalytic site mutant E172A complexed with G5, which is a good substrate for β-amylase, because the rate parameters, K_m and molecular activity, are similar to that of the substrate with a longer chain (*6*). Our results provide a solid basis for understanding the first stage of the hydrolytic reaction of the substrate.

Table 1: Data Collection and Refinement Statistics for the E172A−G5 Complex and the Wild-Type Enzyme−Maltose Complex

	E172A−G5 complex	wild-type enzyme−maltose complex
space group	$P2_1$	$P2_1$
substrate or product	maltopentaose (50 mM)	maltose (50 mM)
cell dimensions		
a, *b*, *c* (Å)	57.20, 90.29, 64.98	56.81, 89.33, 65.39
β (deg)	101.74	102.32
completeness (%) (overall/ outermost shell)	99.4/99.1 (2.21−2.10)	99.9/100.0 (2.11−2.00)
R_{meas}[a] (overall/ outermost shell)	0.080/0.230 (2.21−2.10)	0.056/0.183 (2.11−2.00)
resolution (Å)	30.0−2.10	29.0−2.00
no. of reflections	37458	43133
no. of non-hydrogen atoms		
protein	4115	4119
glucose residue	336	192
calcium	1	1
sulfate	5	5
acetate	8	8
solvent	415	395
R-factor	0.178	0.181
R_{free}	0.212	0.221
rms deviations from ideal values		
bond lengths (Å)	0.007	0.005
bond angles (deg)	1.30	1.30
dihedral angles (deg)	22.20	21.90
improper angles (deg)	0.82	0.82
Ramachandran plot		
most favored (%)	86.9	87.5
allowed (%)	13.1	12.5

[a] $R_{meas} = \sum_h [n_h/(n_h - 1)]^{1/2} \sum_i |I_h - I_{h,i}| / \sum_h \sum_i I_{h,i}$, where n_h, I_h, and $I_{h,i}$ are the multiplicity, intensity, and *i*th intensity measurement of reflection *h*, respectively. Values in parentheses are the resolution ranges in angstroms for the outermost shell.

The crystal of E172A complexed with G5 diffracted to 2.10 Å resolution, and the structure was refined to an *R*-factor of 17.8% and an R_{free} of 21.2%. The other structure and refinement statistics are listed in Table 1. The overall fold of the E172A−G5 complex was almost identical to that of the free enzyme (Figure 1) (*12*), but a large movement of the segment of residues 93−97 (the flexible loop) on loop L3 lying over the active site in the E172A−G5 complex was in a closed form, in contrast to the free enzyme which is in an open form. Saccharides were observed at four locations on the enzyme molecule. One of them was located at the active site in domain A, which consists of a $(\beta/\alpha)_8$ barrel, and the other three were bound at sites located in domain C (Site 1) and domain B (Sites 2 and 3). At the active site, a clear connected density corresponding to a pentasaccharide was observed, the $F_o - F_c$ difference density clearly showed the G5, and each glucose residue could readily be built into the density. The $2F_o - F_c$ density of G5 in the active site is shown in Figure 2a. The five glucose residues in G5 are numbered 1−5 from the nonreducing end (i.e., Glc1−Glc5).

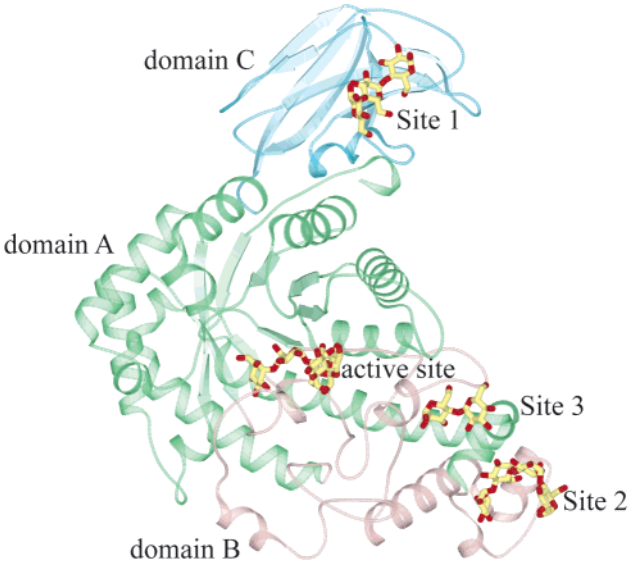

FIGURE 1: Ribbon representation of the E172A−G5 complex. Domains A−C are shown in green, pink, and blue, respectively. A yellow and red stick model represents the maltosaccharides, which bind at the active site and Sites 1−3. This figure was generated using Bobscript (*47*) and RENDER from the raster3D package (*48*).

The average *B*-factors for Glc1−Glc5 were 14.0, 15.3, 14.8, 19.0, and 28.6 Å^2, respectively. They were comparable to those of the surrounding amino acid residues, suggesting full occupancy of G5. All glucose residues adopted a relaxed $^4C_1$ conformation, and the conformation of the maltose unit for Glc2 and Glc3 was much different from those for Glc1 and Glc2, Glc3 and Glc4, and Glc4 and Glc5. The torsion angles around the α-1,4-glucosidic linkage between Glc2 and Glc3 were 145.8° around ϕ (O5−C1−O4′−C4′) and 119.5° around ψ (C1−O4′−C4′−C5′). Although maltooligosaccharides are thought to adopt a relaxed helical conformation, the torsion angles around the α-1,4-glucosidic linkage in the crystal structure of α-maltose were 116° around ϕ and −118° around ψ (*35*). The torsion angles are listed in Table 2 where the subsites in the active site are numbered according to the nomenclature for sugar-binding subsites in glycosyl hydrolase (*36*). The torsion angles are similar to those of the soybean β-amylase−maltose condensation complex reported by Mikami et al. (*8*). Glc1 is almost covered with the flexible loop and has seven hydrogen bonds to four amino acid residues, which is the largest number among other glucose residues, and 14 C−C contacts to eight amino acid residues; Glc2 has three hydrogen bonds to three amino acid residues and 10 C−C contacts to six amino acid residues. In the case of the α-amylase family, an aspartic acid which interacts with O2 and O3 of the glucose residue located at subite −1 is absolutely conserved (*37*−*40*), but in the case of BCM β-amylase, such an amino acid residue could not observed. Glc3 has five hydrogen bonds to three amino acid residues and 16 C−C contacts to eight amino acid residues. Glc4 has only one hydrogen bond to an amino acid residue (His292) and 25 C−C contacts to seven amino acid residues. Glc5 has no direct hydrogen bond and five C−C contacts to two amino acid residues. Most of Glc5 is exposed to solvent. Tables 3 and 4 and Figure 3 show the hydrogen bonding and hydrophobic interactions of the E172A−G5 complex. The interactions between each glucose residue on subsites −2 to +2 and amino acid residues in the active site are almost identical to those of soybean β-amylase−maltose complexes, except for positions Thr330 and Val95 which correspond to Thr342 and Val99 of soybean β-amylase, respectively.

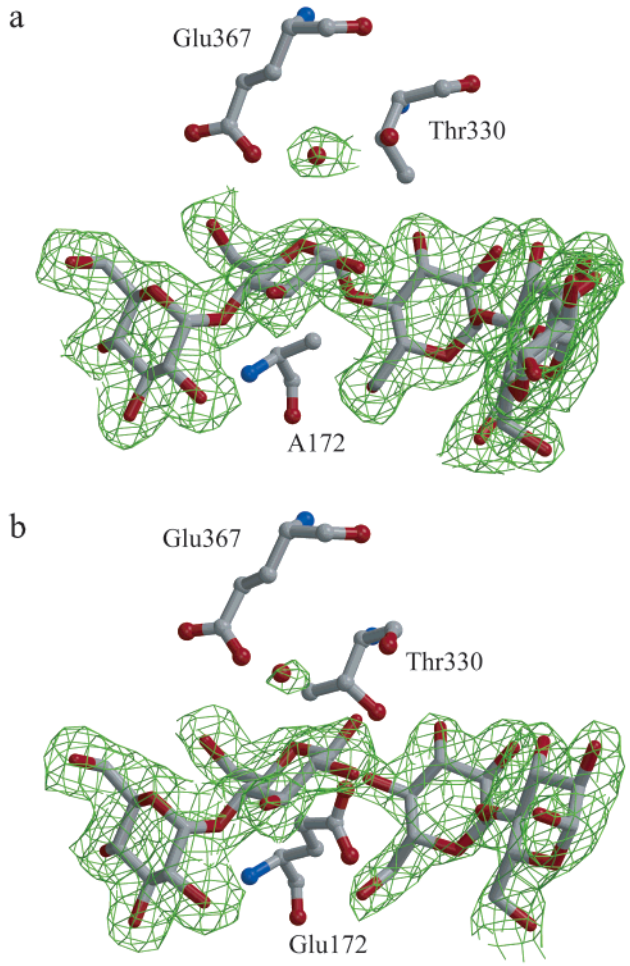

FIGURE 2: Electron density ($2F_o - F_c$) contoured at 1σ for (a) maltopentaose and (b) two maltose molecules, which bind at subsites −2 to +3 of E172A and subsites −2 to +2 of the wild-type enzyme, respectively. Each sugar in panels a and b is shown together with Glu367, Thr330, and Ala172 and with Glu367, Thr330, and Glu172, respectively. This figure was generated using Bobscript (*47*) and RENDER from the raster3D package (*48*).

Table 2: Torsion Angles around the Glucosidic Linkages in the Active Site[a]

	subsites −2 and −1	subsites −1 and +1	subsites +1 and +2	subsites +2 and +3
E172A−G5				
ϕ	70.8	145.8	117.3	105.6
ψ	−148.5	119.5	−105.9	−126.9
wild-type enzyme−maltose				
ϕ	74.9	–	124.0	–
ψ	−154.9	–	−117.6	–
soybean β-amylase−maltose[b]				
ϕ	66.8	152.6	111.7	–
ψ	−151.2	99.8	−112.5	–

[a] ϕ is the O5−C1−O4′−C4′ angle and ψ the C1−O4′−C4′−C5′ angle, where O4 represents the oxygen of the glucosidic linkage, and atoms of the linked reducing end glucose unit are primed. [b] The torsion angles of this enzyme were evaluated by using PDB entry 1BYB. The subsites in the active site are numbered according to the nomenclature for sugar-binding subsites in glycosyl hydrolase (*36*).

Table 3: Hydrogen Bonding Interactions[a] (Å) between Protein and Ligand in the E172A−G5 Complex, the Wild-Type Enzyme−Maltose Complex, and the Soybean β-Amylase−Maltose Complex

sugar atom	amino acid atom	E172A−G5	wild-type enzyme−maltose	soybean β-amylase−maltose[b]
Glc1				
O2	Asp97 OD (101)[c]	2.6	2.5	2.6
O3	His89 NE (93)	2.9	2.8	3.0
O4	Asp49 OD (53)	2.7	2.6	2.6
O4	His89 NE (93)	3.1	2.9	3.0
O5	Arg397 NH (420)	2.9	2.9	3.0
O6	Asp49 OD (53)	2.6	2.5	2.6
O6	Arg397 NH (420)	3.1	2.9	3.1
Glc2				
O1 eq	Thr330 OG1 (342)	ax	3.0	
O1 eq	Thr330 O (342)	ax	2.8	3.3[d]
O1 eq	Glu367 OE (380)	ax		2.8[d]
O1 eq	Asn368 O (381)	ax		2.8[d]
O2	Ala369 O (382)	2.9	2.8	2.8
O3	Val95 O (99)		2.9	
O5	Glu172 OE (186)	*e*	3.2	
O5	Glu367 OE (380)			3.2
O6	Lys287 NZ (295)	3.1	3.0	2.8
O6	Glu367 OE (380)	2.8	3.1	2.8
Glc3				
O2	Gly290 O			
O3	Gly290 N (298)	3.3	3.1	2.9
O3	Thr330 O (342)		3.2	
O3	Thr330 OG (342)		2.8	2.8
O4	Glu172 OE (186)	*e*	2.5	2.6
O4	Thr330 OG (342)		3.1	3.3
O5	Tyr178 OH (192)	3.2	3.1	3.1
O6	Glu172 OE (186)	*e*		2.6
O6	Arg174 NE (188)			3.3
O6	Arg174 NH (188)	3.0		2.9
O6	Tyr178 OH (192)	2.9		2.8
Glc4				
O3	His292 NE (300)	2.9	2.7	2.7

[a] H-bond distance of <3.3 Å for the E172A−G5 complex and the wild-type enzyme−maltose complex. [b] These values are for the soybean β-amylase−200 mM maltose complex taken from PDB entry 1BYB. [c] Numbers in parentheses are soybean β-amylase residue numbers corresponding to those of BCM β-amyalse. [d] These values are for the soybean β-amylase−200 mM maltose complex taken from ref *8*. [e] This residue is replaced with an alanine residue.

Table 4: C−C Contacts between Protein and Ligand in the E172A−G5 Complex, the Wild-Type Enzyme−Maltose Complex, and the Soybean β-Amylase−Maltose Complex

	C−C contact[a]		
sugar residue	E172A−G5	wild-type enzyme−maltose	soybean β-amylase−maltose[b]
Glc1	Met16		
	Leu19	Leu19	Leu20
	Asp49	Asp49	Asp53
	Trp51	Trp51	Trp55
	Ile85	Ile85	Ile89
	His89	His89	
	Asp97	Asp97	Asp101
	Ala170	Ala170	Ala184
Glc2	Val95	Val95	
		Ala170	
	c	Glu172	Glu186
	Lys287	Lys287	Lys295
	Thr330	Thr330	Thr342
	Glu367		
	Ala369	Ala369	Ala382
	Leu396	Ile396	Leu419
Glc3	Val95	Val95	
	Ala170	Ala170	Ala184
	c	Glu172	Glu186
		Arg174	
	Tyr178	Tyr178	Tyr192
	Ala289	Ala289	Ser292
	Gly290	Gly290	Gly298
	Trp293	Trp293	Trp301
	Thr330		
	Ala369	Ala369	Ala382
Glc4	Val95	Val95	Val99
	Tyr178	Tyr178	Tyr192
	Tyr186	Tyr186	Trp198
			Phe200
	His292	His292	His300
	Trp293	Trp293	Trp301
	Met334		Met346
	Leu370	Leu370	Leu383
Glc5	Val95		
	Leu370		

[a] C−C distance of <4.5 Å for the E172A−G5 complex and the wild-type enzyme−maltose complex. [b] These values are for the soybean β-amylase−200 mM maltose complex taken from PDB entry 1BYB. [c] This residue is replaced with an alanine residue.

Structure of the Wild-Type Enzyme Complexed with Maltose. The crystal of the wild-type enzyme complexed with maltose diffracted to 2.00 Å resolution, and the structure was refined to an *R*-factor of 18.1% and an R_{free} of 22.1%. The other structure and refinement statistics are listed in Table 1. The overall fold of the wild-type enzyme−maltose complex was almost identical to that of the E172A−G5 complex. Maltose was observed at four sites on the enzyme molecule: two maltoses were bound at subsites −2 to +2 in tandem, and the others were bound at Site 1 and Site 2. Electron density was observed between Glc2 and Glc3 in the active site (Figure 2b). The electron density of Glc2 suggests the existence of α- and β-maltose. When α- or β-maltose binds at subsites −2 and −1, the other maltose molecule cannot bind to subsites +1 and +2 at the same time because the distance between the C1 atom of Glc2 and the O4 atom of Glc3 is too short (1.7 Å), unless a condensation between the maltose molecules occurs. The average *B*-factors for Glc1−Glc4 at the active site were 24.4, 44.4, 51.4, and 54.0 Å^2, respectively. They are higher than those of the E172A−G5 complex, and the average *B*-factor of the maltose at subsites +1 and +2 was higher than others. Also, the average *B*-factor of the flexible loop was 1.3-fold higher than that of the E172A−G5 complex. These facts suggest that a maltose molecule alternatively binds at subsites −2 and −1, or at subsites +1 and +2. Figure 4 shows a comparison of the conformations of sugar in the wild-type enzyme and other enzymes (i.e., soybean β-amylase, E172A, and β-amylase BQ10-S1). As shown in Figure 4a, the conformations of maltose molecules in the wild-type enzyme are quite similar to those of the soybean β-amylase−maltose complex; however, the conformation of the maltose that occupied subsites +1 and +2 is different from that in the E172A−G5 complex or in the complex of β-amylase from *B. cereus* BQ10-S1 SpoII (BQ10-S1) and maltose (*13*). As shown in Figure 4b, the position of the C4 atom of Glc3 in the wild-type enzyme−maltose complex shifted 0.7 Å toward the side chain of Ala289 compared with that in the E172A−G5 complex, the position of the C4 atom of Glc3 in the BQ10-S1 β-amylase−maltose complex shifted 1.1 Å, and the Glc3 slid toward Glc4 compared with that of the wild-

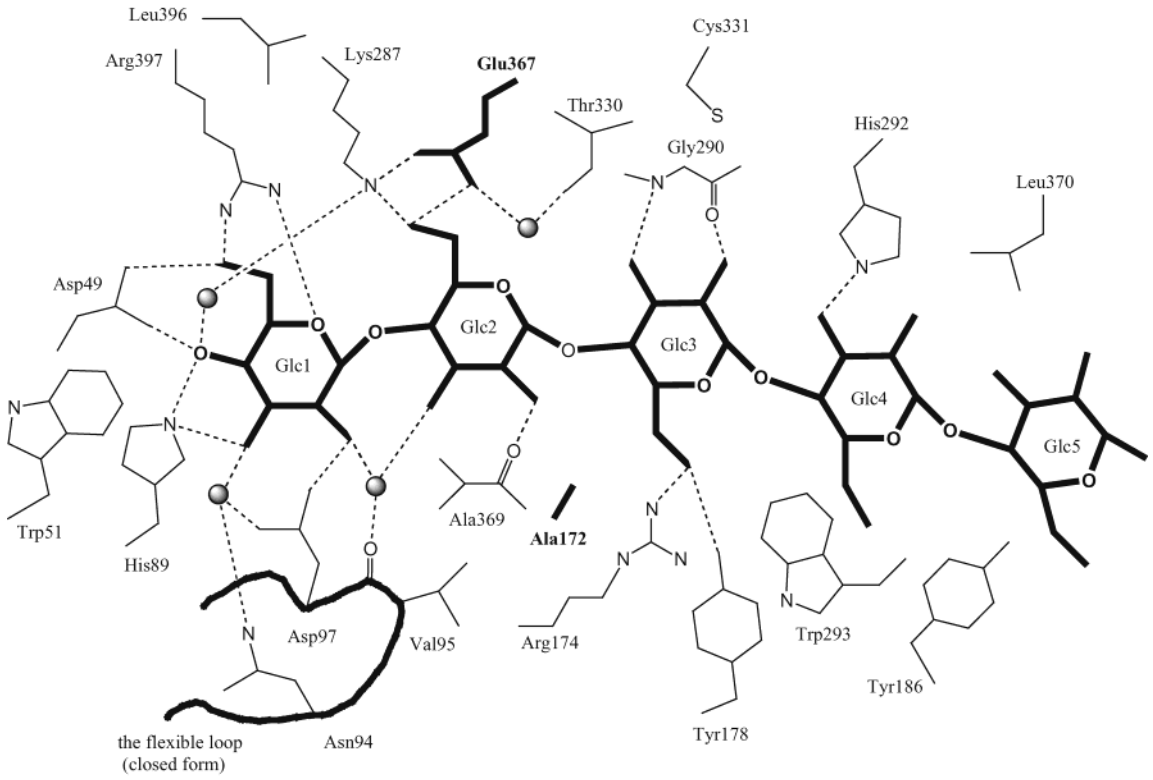

FIGURE 3: Schematic drawing of the binding mode of a substrate, G5, in the active site of the E172A−G5 complex. Water molecules are presented as gray spheres. Possible hydrogen bonds are represented with dashed lines. This figure was generated using Bobscript (*47*) and RENDER from the raster3D package (*48*).

type enzyme−maltose complex (see Figure 4c). The distance between the C1 atom of Glc2 and the O4 atom of Glc3 in the BQ10-S1 β-amylase−maltose complex is 3.0 Å, which differs from that of the wild-type enzyme−maltose complex (1.7 Å). Thr330 and Cys331 on loop L6 in the wild-type enzyme−maltose complex shifted toward Glc3 so that the distance between the OG atom of Thr330 and the O3 atom of Glc3 was 2.7 Å as in the soybean β-amylase−maltose complex (*8*), the BQ10-S1 β-amylase−maltose complex (*13*), and the BCM β-amylase−GGX complex (*14*). Consequently, a hydrogen bond was formed. In the case of the E172A−G5 complex, however, such a shift was not observed and the conformations of Thr330 and Cys331 were identical to those of the free enzyme (*12*) (see Figure 4b).

Other Binding Sites. The enzyme has a starch binding domain (domain C) similar to those of CGTase (*15*) and glucoamylase (*16*). Electron densities corresponding to a trisaccharide in the E172A−G5 complex and to a maltose in the wild-type enzyme−maltose complex were observed at Site 1 in domain C (Figure 1). The conformation of two glucose residues from the reducing end of the trisaccharide in the E172A−G5 complex was almost identical to that of the maltose in the wild-type enzyme−maltose complex, which interact with four residues, Trp449, Trp495, Gln499, and Lys482. In particular, the two glucose residues were bound to Trp449 and Trp495 by a stacking interaction. The interaction is quite similar to that in the BQ10-S1 β-amylase−maltose complex reported by Mikami et al. (*13*). The nonreducing end glucose residue has only a C−C contact with Trp449 and no hydrogen bonding with amino acid residues. The reducing end in the wild-type enzyme−maltose complex was a β-anomer, but that of the E172A−G5 complex was an α-anomer.

Two binding sites were found in domain B in the E172A−G5 complex (Figure 1). One is located in the same place as the BCM β-amylase−GGX complex at Site 2 (*14*), and electron density corresponding to a tetrasaccharide with a relaxed helical conformation was observed on the molecular surface. The conformation of two glucose residues from the nonreducing end of the tetrasaccharide was identical to those of the wild-type enzyme−maltose complex and the BCM β-amylase−GGX complex. The reducing end in the wild-type enzyme−maltose complex was a β-anomer, but that of the E172A−G5 complex was an α-anomer. A new electron density corresponding to one disaccharide in the E172A−G5 complex was observed at Site 3, located ~14 Å from the glucose residue of the reducing end of G5 bound at the active site. The nonreducing end glucose residue had four hydrogen bonds to three amino acid residues and 15 C−C contacts (Glu238, Asn297, Thr299, Ile300, Tyr340, and Tyr343). The reducing end glucose residue had three hydrogen bonds to three amino acid residues and 12 C−C contacts to five amino acid residues (Ser188, Arg189, Gln294, Asn297, Ile300, Tyr340, and Pro341), and the O1 atom exhibited the α-configuration. As the reducing end glucose residues at Sites 1−3 in the E172A−G5 complex exhibited α-configurations and the E172A lost activity (*19*), it is suggested that G5 was bound at each binding site.

In the case of cyclodextrin glycosyltransferase from *Bacillus circulans* strain 251, the maltose binding Site 2 (MBS2) is situated at the beginning of the groove leading to the active site, suggesting a role for MBS2 in guiding the substrate to the active site (*41*). The binding site corresponding to MBS2 was not observed in domain C of BCM β-amylase, and all nonreducing ends of saccharides at the binding sites did not directly face the active site. All binding

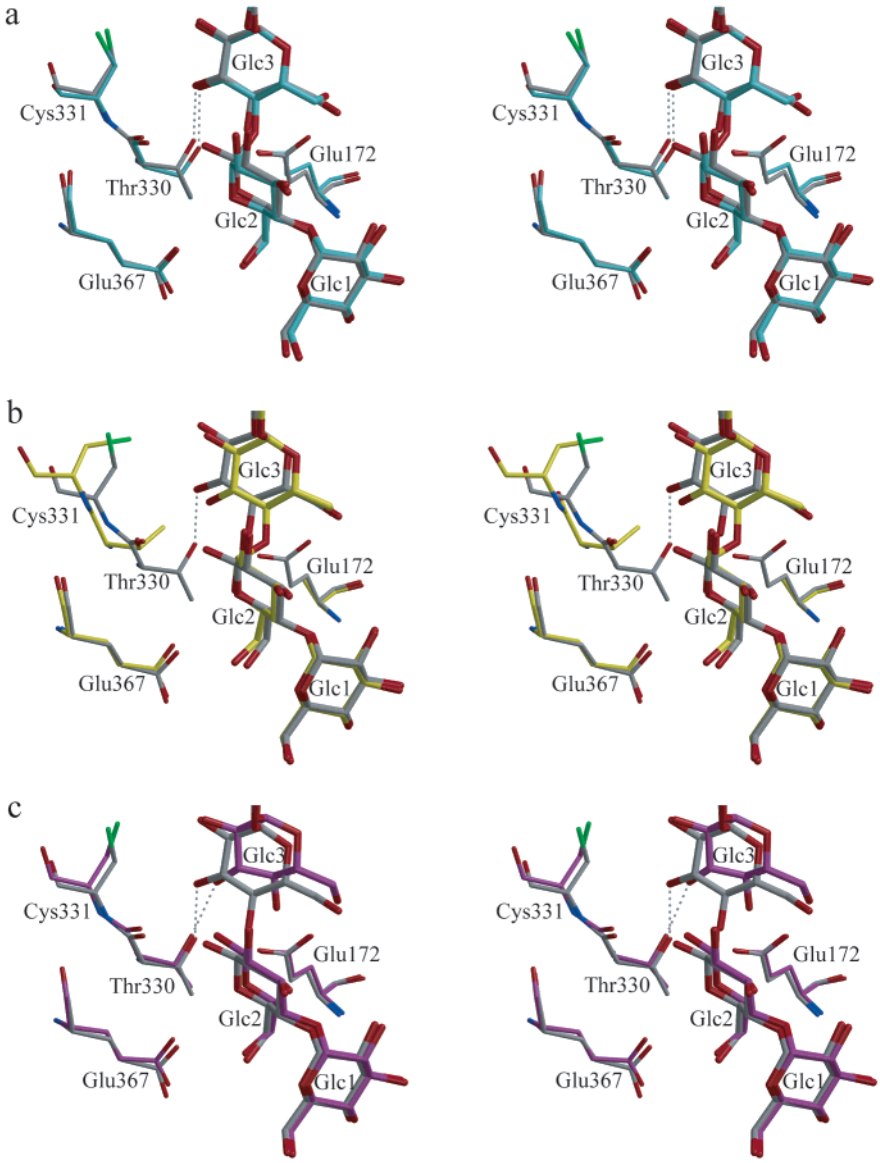

FIGURE 4: Stereorepresentations of the superposition of the enzyme−sugar complex: (a) wild-type enzyme−maltose complex in gray and soybean β-amylase−maltose complex (PDB entry 1BYB) in cyan, (b) wild-type enzyme−maltose complex in gray and E172A−G5 complex in yellow, and (c) wild-type enzyme−maltose complex in gray and BQ10-S1 β-amylase−maltose complex (PDB entry 1B9Z) in purple.

sites were observed on a half-surface of the enzyme molecule containing the active site (see Figure 5a); however, no binding site was observed on the opposite surface (see Figure 5b). Thus, it is thought that the binding site (Sites 1−3) simply plays the role of adsorbing to the surface of raw starch.

Catalytic Mechanism of BCM β-Amylase. In the crystal of the E172A−G5 complex, G5 was not hydrolyzed. It seems that the structure of the E172A−G5 complex corresponds to a Michaelis complex which is a noncovalent enzyme−substrate complex (ES complex) in the reaction coordinate for the wild-type enzyme. In the wild-type enzyme−maltose complex, two maltose molecules occupied subsites −2 to +2 by the same binding conformation as G5 in the E172A−G5 complex. The catalytic residues Glu172 and Glu367 are located between subsites −1 and +1. We demonstrated that Glu367 acts as general base and Glu172 acts as general acid in the previous study on the chemical rescue of a catalytic site mutant E367A by azide (*19*); thus, it is confirmed that the pK_a's of Glu172 and Glc367 in the free enzyme are 8.4 and 4.0, respectively (*6*).

In the E172A−G5 complex, a water molecule was observed 3.0 and 3.3 Å from the OE1 atom of Glu367 and the C1 atom of Glc2, respectively (see Figure 2a). In the case of the wild-type enzyme−maltose complex, $F_o - F_c$ electron density of the water molecule was also observed at almost the same place as in the E172A−G5 complex. However, the positive peak of the $2F_o - F_c$ electron density is not as strong as that of the E172A−G5 complex. The fact that Glc2 also exhibits the β-anomer suggests that it is difficult for the water molecule to fit in this place. The carboxyl group (COO^-) of Glu367 can activate the coordinated water molecule (between the OE1 atom of Glu367 and the C1 atom of Glc2) in either SN1 or SN2 reactions, and the hydroxide ion generated from the water molecule activated by the OE1 atom of Glu367 can act as a nucleophile toward the C1 atom of Glc2 so that β-maltose is produced.

The conformation of the substrate that binds to the active site is very important in understanding the mechanism of the catalytic reaction. The distance between the O2 atom of Glc2 and the O3 atom of Glc3 is 3.9 Å due to rotation of

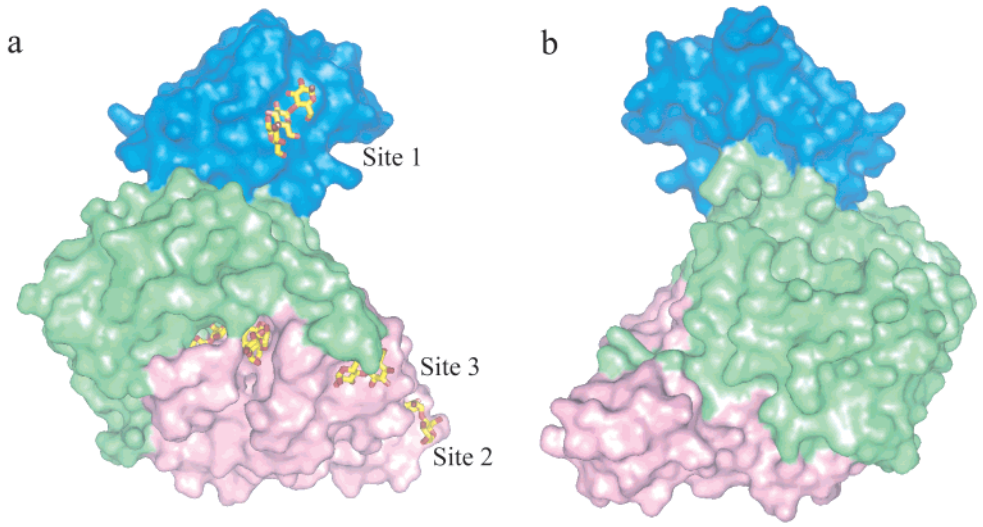

FIGURE 5: Surface models of the E172A−G5 complex using Pymol (http://www.pymol.org). Model b is the other side of model a, rotated 180°. A yellow and red stick model represents the maltosaccharides, which bind at the active site and Sites 1−3. Domains A−C are shown in green, pink, and blue, respectively.

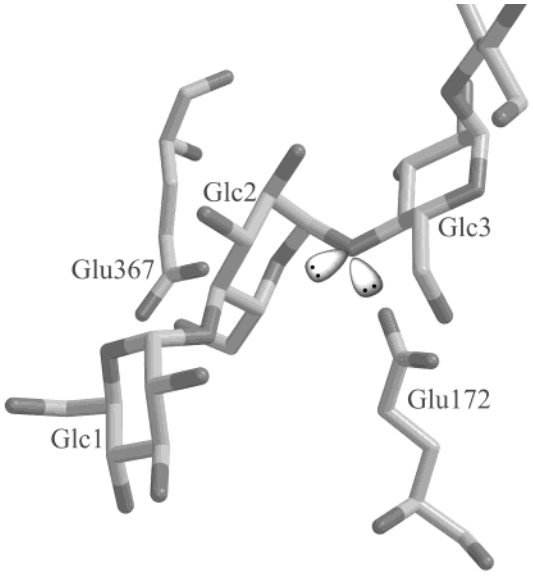

FIGURE 6: Orientation of the α-1,4-glucosidic bond between Glc2 and Glc3 of G5 at the catalytic site of BCM β-amylase. Main chains of E172A−G5 and wild-type enzyme−maltose complexes are superimposed. G5, Glu367 of the E172A−G5 complex, and Glu172 of the wild-type enzyme−maltose complex are shown as stick model. The lobes of the orbital show lone pair electrons.

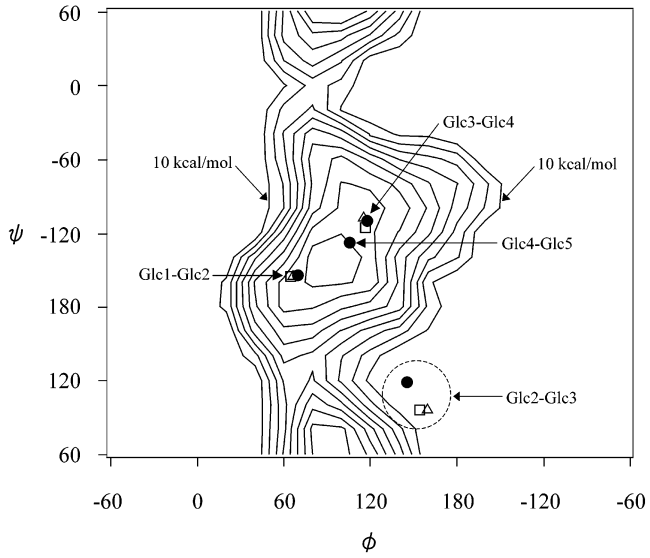

FIGURE 7: Distribution of glucosidic dihedral angles ϕ and ψ for maltose, in which the MM3 isoenergy contours are calculated with an ϵ of 4 (*45*): (●) E172A−G5 complex, (□) soybean β-amylase−200 mM maltose complex, and (△) soybean β-amylase−8 mM maltose complex. The torsion angles of soybean β-amylase were evaluated by using PDB entries 1BYB and 1BYC.

the glucosidic bond between Glc2 and Glc3; thus, there is no interaction between them as in the case of the α-amylase family (*22*, *40*). In the case of CGTase, which catalyzes both hydrolysis and transglycosylation reactions (*42*), it is suggested that the rotation of the glucosidic bond facilitates departure of the leaving group after formation of the intermediate (*40*). In the case of β-amylase, however, it is not necessary to depart the leaving group because β-amylase catalyzes a hydrolytic reaction but does not do a transglycosylation reaction. The hydrolytic reaction should be able to occur with facility as a water molecule exists between the C1 atom of the reactive pyranose ring and OE1 of Glu367 acting as a nucleoplile (see Figure 2a), even if a substrate occupies subsites −2 to +3 and the leaving group does not depart from the catalytic site. On the other hand, the rotation of a glucosidic bond positions a lone pair of the O4′ atom in the direction of Glu172 acting as a proton donor as shown in Figure 6. This allows lateral protonation of the glucosidic oxygen atom and will be advantageous for providing a proton from Glu172 to glucosidic oxygen. Such an orientation has been discussed for retaining enzymes (*40*, *43*, *44*).

In the E172A−G5 complex, the conformation of the maltose unit for Glc2 and Glc3 was much different from other maltose units. All torsion angles of the α-1,4-glucosidic linkage are shown as empty circles on a Ramachandran-like plot for maltose (Figure 7), in which the MM3 isoenergy contours calculated with an ϵ of 4 (*45*) are shown by the solid curves. All ϕ and ψ values except one correspond to those of the *cis* conformation ($\phi = 93°$, $\psi = -145°$) which is the most stable in solution. However, the substrate flips between Glc2 and Glc3, and the conformational energy of this maltose unit is 20 kcal/mol higher than that of the *cis* conformation. It is interesting that maltotetraose binds to

soybean β-amylase in the same conformation as Glc1−Glc4 of G5 to BCM β-amylase. Also, the maltose unit which includes the glucosidic linkage to be broken has a higher conformational energy: $\phi = 152.6°$ and $\psi = 99.8°$ (a regular square in dot circles in Figure 7). Thus, the glucosidic linkage between Glc2 and Glc3 appears to be strained on binding, but the energy required to form this unfavorable conformation could easily be overcome by numerous enzyme−substrate interactions, including the movement of the flexible loop (Tables 3 and 4 and Figure 3). These interactions between the enzyme and substrate are seen to be in good agreement with those of maltotetraose (condensation product) in the soybean β-amylase−maltose complex. Computer simulations to explain how these interactions stabilize the substrate are in progress. Kaneko et al. (*46*) analyzed the structure of the soybean β-amylase−maltotetraose complex and explained the rotation of the substrate between Glc2 and Glc3. By this rotation, β-amylase makes the substrate bind in such a way that its glucosidic oxygen is pointing toward the bottom of the active cleft, avoiding the collision of the substrate with the cleft. Then, a water molecule attacks the intermediate from the exit of the cleft to produce only the β-anomer. In addition to their suggestion, we suggest here that β-amylase destabilizes the bond that is to be broken in the ES complex, decreasing the activation energy, $\Delta G^{\ddagger}$, which is the difference in free energy between this state and the transition state. As a result, β-amylase could catalyze the hydrolysis of amylose, producing the β-anomer of maltose.

NOTE ADDED AFTER ASAP POSTING

This paper was posted prematurely on the Web on 04/18/03. β-Amylase is now correctly identified as belonging to only family 14 in the second sentence of the text. The corrected version of this paper was posted 04/22/03.

ACKNOWLEDGMENT

We thank Drs. N. Igarashi, M. Suzuki, and N. Sakabe for the technical assistance at the Photon Factory.

REFERENCES

1. Henrissat, B., and Davis, G. (1997) *Curr. Opin. Struct. Biol. 7*, 637−644.
2. Toda, H., Nitta, Y., Asanami, S., Kim, J. P., and Sakiyama, F. (1993) *Eur. J. Biochem. 216*, 25−38.
3. Nitta, Y., Tomita, K., Kohno, M., Nakashima, T., and Matsumoto, Y. (1991) *Denpun Kagaku 38*, 159−164.
4. Suganuma, T., Ohnishi, M., Hiromi, K., and Morita, Y. (1980) *Agric. Biol. Chem. 44*, 1111−1117.
5. Kato, M., Hiromi, K., and Morita, Y. (1974) *J. Biochem. 75*, 563−576.
6. Nitta, Y., Shirakawa, M., and Takasaki, Y. (1996) *Biosci., Biotechnol., Biochem. 60*, 823−827.
7. Mikami, B., Hehre, E. J., Sato, M., Katsube, Y., Hirose, M., Morita, Y., and Sacchettini, J. C. (1993) *Biochemistry 32*, 6836−6845.
8. Mikami, B., Degano, M., Hehre, E. J., and Sacchettini, J. C. (1994) *Biochemistry 33*, 7779−7787.
9. Adachi, M., Mikami, B., Katsube, T., and Utsumi, S. (1998) *J. Biol. Chem. 273*, 19859−19865.
10. Cheong, C. G., Eom, S. H., Chang, C., Shin, D. H., Song, H. K., Min, K., Moon, J. H., Kim, K. K., Hwang, K. Y., and Suh, S. W. (1995) *Proteins 21*, 105−117.
11. Mikami, B., Yoon, H. J., and Yoshigi, N. (1999) *J. Mol. Biol. 285*, 1235−1243.
12. Oyama, T., Kusunoki, M., Kishimoto, Y., Takasaki, Y., and Nitta, Y. (1999) *J. Biochem. 125*, 1120−1130.
13. Mikami, B., Adachi, M., Kage, T., Sarikaya, E., Nanmori, T., Shinke, R., and Utsumi, S. (1999) *Biochemistry 38*, 7050−7061.
14. Oyama, T., Miyake, H., Kusunoki, M., and Nitta, Y. (2002) *J. Biochem. 133* (in press).
15. Lawson, C. L., van Montfort, R., Strokopytov, B., Rozeboom, H. J., Kalk, K. H., de Vries, G. E., Penninga, D., Dijkhuizen, L., and Dijkstra, B. W. (1994) *J. Mol. Biol. 236*, 590−600.
16. Sorimachi, K., Jacks, A. J., Le Gal-Coeffet, M. F., Williamson, G., Archer, D. B., and Williamson, M. P. (1996) *J. Mol. Biol. 259*, 970−987.
17. Isoda, Y., and Nitta, Y. (1986) *J. Biochem. 99*, 1631−1637.
18. Nitta, Y., Isoda, Y., Toda, H., and Sakiyama, F. (1989) *J. Biochem. 105*, 573−576.
19. Miyake, H., Otsuka, C., Nishimura, S., and Nitta, Y. (2002) *J. Biochem. 131*, 587−591.
20. Yoshioka, Y., Hasegawa, K., Matsuura, Y., Katsube, Y., and Kubota, M. (1997) *J. Mol. Biol. 271*, 619−628.
21. Hasegawa, K., Kubota, M., and Matsuura, Y. (1999) *Protein Eng. 12*, 819−824.
22. Fujimoto, Z., Takase, K., Doui, N., Momma, M., Matsumoto, T., and Mizuno, H. (1998) *J. Mol. Biol. 277*, 393−407.
23. Knegtel, R. M., Strokopytov, B., Penninga, D., Faber, O. G., Rozeboom, H. J., Kalk, K. H., Dijkhuizen, L., and Dijkstra, B. W. (1995) *J. Biol. Chem. 270*, 29256−29264.
24. Uitdehaag, J. C., Kalk, K. H., van Der Veen, B. A., Dijkhuizen, L., and Dijkstra, B. W. (1999) *J. Biol. Chem. 274*, 34868−34876.
25. Uitdehaag, J. C., van Alebeek, G. J., van Der Veen, B. A., Dijkhuizen, L., and Dijkstra, B. W. (2000) *Biochemistry 39*, 7772−7780.
26. Uitdehaag, J. C., Mosi, R., Kalk, K. H., van der Veen, B. A., Dijkhuizen, L., Withers, S. G., and Dijkstra, B. W. (1999) *Nat. Struct. Biol. 6*, 432−436.
27. McPhaerson, A. (1982) *Preparation and Analysis of Protein Crystals*, 1st ed., pp 96−97, John Wiley, New York.
28. Stura, E. A., and Wilson, I. A. (1992) A Practical Approach, in *Crystallization of Nucleic Acids and Proteins* (Ducruix, A., and Giege, R., Eds.) pp 99−126, IRL Press, Oxford, U.K.
29. Rossmann, M. G., and van Beeek, C. G. (1999) *Acta Crystallogr. D55*, 1631−1640.
30. Collaborative Computational Project Number 4 (1994) *Acta Crystallogr. D50*, 760−763.
31. Navaza, J. (1994) *Acta Crystallogr. A50*, 157−163.
32. Brunger, A. T., Adams, P. D., Clore, G. M., DeLano, W. L., Gros, P., Grosse-Kunstleve, R. W., Jiang, J. S., Kuszewski, J., Nilges, M., Pannu, N. S., Read, R. J., Rice, L. M., Simonson, T., and Warren, G. L. (1998) *Acta Crystallogr. D54*, 905−921.
33. Brunger, A. T. (1992) *Nature 355*, 472−474.
34. Jones, T. A., Zou, J. Y., Cowan, S. W., and Kjeldgaard, M. (1991) *Acta Crystallogr. A47*, 110−119.
35. Takusagawa, F., and Jacobson, R. A. (1978) *Acta Crystallogr. B34*, 213−218.
36. Davies, G. J., Wilson, K. S., and Henrissat, B. (1997) *Biochem. J. 321*, 557−559.
37. Matsuura, Y., Kusunoki, M., Harada, W., and Kakudo, M. (1984) *J. Biochem. 95*, 697−702.
38. Strokopytov, B., Penninga, D., Rozeboom, H. J., Kalk, K. H., Dijkhuizen, L., and Dijkstra, B. W. (1995) *Biochemistry 34*, 2234−2240.
39. Brzozowski, A. M., and Davies, G. J. (1997) *Biochemistry 36*, 10837−10845.
40. Uitdehaag, J. C., van Der Veen, B. A., Dijkhuizen, L., and Dijkstra, B. W. (2002) *Enzymol. Microb. Technol. 30*, 295−304.
41. Penninga, D., van der Veen, B. A., Knegtel, R. M., van Hijum, S. A., Rozeboom, H. J., Kalk, K. H., Dijkstra, B. W., and Dijkhuizen, L. (1996) *J. Biol. Chem. 271*, 32777−32784.
42. van der Veen, B. A., van Alebeek, G. J., Uitdehaag, J. C., Dijkstra, B. W., and Dijkhuizen, L. (2000) *Eur. J. Biochem. 267*, 658−665.
43. Heightman, T. D., and Vasella, A. T. (1999) *Angew. Chem., Int. Ed. 38*, 750−770.
44. Varrot, A., Schülein, M., Pipelir, M., Vasella, A., and Dacies, G. J. (1999) *J. Am. Chem. Soc. 121*, 2621−2622.
45. Shimada, J., Kaneko, H., Takada, T., Kitamura, S., and Kajiwara, K. (2000) *J. Phys. Chem. B 104*, 2136−2147.
46. Kaneko, H., Kuriki, T., Handa, S., Takada, T., Takata, H., Yanase, M., Okada, S., Umeyama, H., and Shimada, J. (1998) *Res. Commun. Biochem. Cell Mol. Biol. 2*, 69−89.
47. Esonuf, R. M. (1997) *J. Mol. Graphics 15*, 132−134.
48. Merritt, E. A., and Murphy, M. E. P. (1994) *Acta Crystallogr. D50*, 869−873.

BI020712X